

# Pd<sub>8</sub> Cluster: Too Small to Melt? A BOMD Study

Analila Luna-Valenzuela, Jesús N. Pedroza-Montero, Andreas M. Köster, Patrizia Calaminici, Luis E. Gálvez-González, and Alvaro Posada-Amarillas\*

 Cite This: <https://doi.org/10.1021/acs.jpca.3c06173>

 Read Online

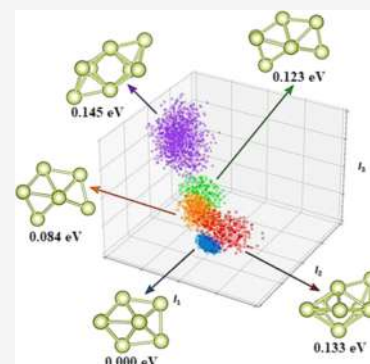
ACCESS |

 Metrics & More

 Article Recommendations

 Supporting Information

**ABSTRACT:** The question of whether a solid–liquid phase transition occurs in small clusters poses a fundamental challenge. In this study, we attempt to elucidate this phenomenon through a thorough examination of the thermal behavior and structural stability of Pd<sub>8</sub> clusters employing ab initio simulations. Initially, a systematic global search is carried out to identify the various isomers of the Pd<sub>8</sub> cluster. This is accomplished by employing an ab initio basin-hopping algorithm and using the PBE/SDD scheme integrated in the Gaussian code. The resulting isomers are further refined through reoptimization using the deMon2k package. To ensure the structural firmness of the lowest-energy isomer, we calculated normal modes. The structural stability as a function of temperature is analyzed through the Born–Oppenheimer molecular dynamics (BOMD) approach. Multiple BOMD trajectories at distinct simulated temperatures are examined with data clustering analysis to determine cluster isomers. This analysis establishes a connection between the potential energy landscape and the simulated temperature. To address the question of cluster melting, canonical parallel-tempering BOMD runs are performed and analyzed with the multiple-histogram method. A broad maximum in the heat capacity curve indicates a melting transition between 500 and 600 K. To further examine this transition, the mean-squared displacement and the pair-distance distribution function are calculated. The results of these calculations confirm the existence of a solid–liquid phase transition, as indicated by the heat capacity curve.



## 1. INTRODUCTION

The physical and chemical properties of nanoparticles are radically different from those of crystalline bulk solids, varying as a function of size, shape, chemical ordering, and composition.<sup>1</sup> The scientific interest generated by these entities is due to their current and potential technological applications, such as industrial catalysis for refinement of petroleum, control of pollution, drug synthesis, etc.,<sup>2</sup> as to the bridge they represent for the study and understanding of materials at the nanoscale level.<sup>3</sup> In general, when dealing with nanoscale materials, catalysis presents a number of complex scenarios; the simplest one considers free clusters interacting with specific molecules. At this size scale, experimental studies require theoretical support to gain an atomistic understanding of the observed cluster response to external stimuli. In this regard, different theoretical approaches have been implemented to attain the chemical and physical properties of clusters and nanoparticles at  $T = 0$  K. In the past few years, several investigations have also explored the structural properties at higher temperatures from an ab initio viewpoint, thus improving the accuracy of results regarding similar studies carried out using empirical potentials.<sup>4</sup> In many cases, the initial structures required for the implementation of high-temperature studies are obtained from global optimization approaches employing electronic structure methods.

Overall, a potential energy surface (PES) exploration is necessary as a starting point to obtain a set of stable structures of clusters, the isomers, which are identified by both geometry and

energy, thus obtaining the corresponding energetical ordering. However, the complexity of the PES of metal clusters and the associated high computational cost of performing ab initio global explorations pose a remarkable obstacle. Despite these challenges, research on the design and use of global optimization algorithms dedicated to the PES exploration of clusters has seen notable advances over the past years. For instance, the works by Schön et al.<sup>5</sup> Doye and Wales,<sup>6</sup> Heiles and Johnston,<sup>7</sup> and Lourenço et al.<sup>8</sup> are inspiring examples that have employed empirical and ab initio schemes to perform extensive global optimization searches to locate the different minima of a PES. Most interestingly, recent experimental and theoretical studies have shed some light on the structural stability of the located minimum-energy structures through the analysis of the energy barriers among the different isomer structures.<sup>9–11</sup> Foster et al.<sup>9</sup> determined the energy difference between isomers of gold nanoparticles at low (20–125 °C) and high (125–500 °C) temperatures, in both cases observing cluster structural rearrangements between different symmetries. Maneri et al.<sup>10</sup> performed BOMD simulations at finite temperatures to analyze

**Received:** September 13, 2023

**Revised:** December 20, 2023

**Accepted:** December 28, 2023

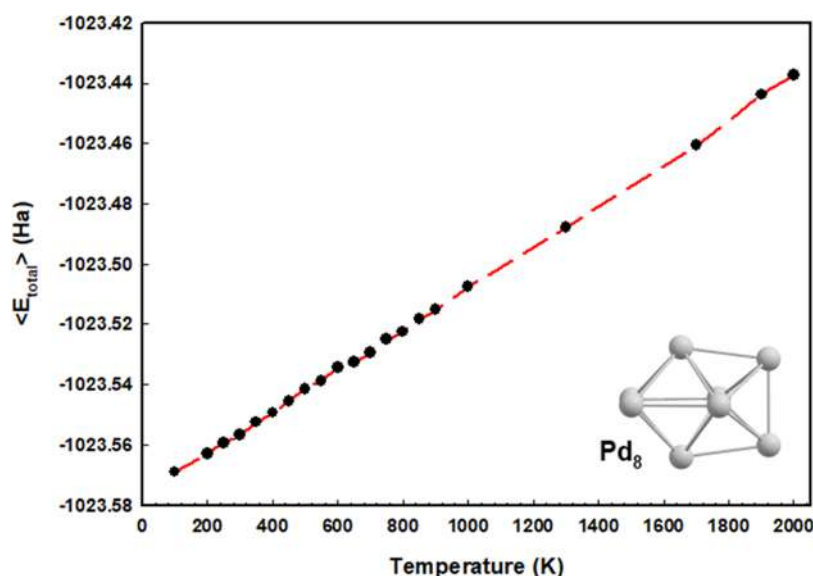


**Figure 1.** Caloric curve for the Pd<sub>8</sub> cluster obtained from the BOMD trajectory data. The lowest-energy cluster geometry corresponds to a trigonal (Siamese) dodecahedron. Cartesian coordinates are provided in [Supporting Information](#).

the thermal stability of small Si–B clusters, while Fiscaro et al.<sup>11</sup> have discussed the principles underlying the structural stability of metal clusters, identifying that these clusters find their ground state by crossing low energy barriers.

A second issue appears in realistic studies, which must take into account the temperature, a major determinant of the structural changes and with significant influence on the properties of metal clusters. In this case, the problem requires dealing with computer simulation schemes suitable to work out the thermodynamics of small systems, such as empirical potential (EP) and ab initio molecular dynamics (MD) simulations. In EP MD, several examples contextualizing this method are found in the literature.<sup>12–14</sup> The structural response of clusters to temperature has been revealed by Garzón et al.<sup>12</sup> in the Au<sub>38</sub> cluster, and by Cabrera-Trujillo et al.,<sup>13</sup> who analyzed the structural fluctuations in Au clusters. They provided evidence of the appearance of different isomers as the temperature rises. Sanders-Gutierrez et al.<sup>14</sup> carried out molecular dynamics simulation on 38-atom coinage metal clusters, determining, among other properties, the melting temperature of the corresponding lowest-energy configuration. More recently, the heat transfer mechanisms of Ag–Au and Ag–Pd nanoparticles were thoroughly studied through MD simulations,<sup>15</sup> finding a nonmonotonous behavior of thermal conductivity as a function of Au and Pd content, and a significant phonon and diffusion contribution at high temperature.

Unlike EP methods, the computational demands inherent to quantum mechanical methodologies, such as ab initio molecular dynamics (AIMD), impose limitations on their applicability for the investigation of nanoparticles or larger systems.<sup>16,17</sup> However, this is not a drawback in the study of metal clusters. This is mainly because the physicochemical properties relevant to practical applications, such as the promotion of chemical reactions by modification of the rate of reaction,<sup>18</sup> have their origin in this subnanometer-size regime, where quantum phenomena are dominant. Furthermore, at this size, EPs fail to predict the correct structure because the decisive quantum variables needed are not explicit in the analytical form of the EP. In this regard, considerable advances in the AIMD methods have been achieved with the aim of studying transition and noble

metal clusters<sup>10,12,13,19,21–23</sup> employing the more advanced AIMD methods. Successful applications of the BOMD method are described by Calaminici et al.<sup>19</sup> employing the auxiliary density functional theory (ADFT) scheme implemented in the deMon2k package.<sup>20</sup> The finite temperature behavior of Na and Au clusters has been exhaustively analyzed using this approach.<sup>21–26</sup> Of these, the works carried out to determine the melting point of Au clusters<sup>21</sup> and the specific heat of Na clusters<sup>24,26</sup> stand out. The strategies used there are now routine work to perform similar analyses, as can be seen in the referred works. A different approach using the AIMD method has been implemented by Sun and Cheng<sup>27</sup> and Fan et al.<sup>28</sup> to study the temperature dependence of Au and Cu cluster catalysts. Other density functional theory (DFT) methods, such as finite temperature (FT-DFT)<sup>29</sup> or thermally assisted-occupation (TAO–DFT)<sup>30</sup> approaches, are not considered in this research.

Previous studies have demonstrated that the melting behavior of subnanometric clusters differs from those of their bulk counterparts. Furthermore, determining phase transitions in such small structures can be a complex and ambiguous task.<sup>31</sup> Nevertheless, there is a consensus about using the average total energy as a function of the temperature, known as the caloric curve, as an effective method to estimate and identify phase transitions. In this approach, the caloric curve exhibits three well-defined regions as temperature increases, and the following interpretation has been given. For low and high temperatures, a linear behavior of total energy vs temperature is observed, and at an intermediate region, where clusters in different phases coexist, a jump in total energy is perceptible in a range of temperatures.

From the molecular dynamics simulation viewpoint, the initial geometric structure is well defined, which at low temperatures undergoes only small distortions, and the solid-like phase persists. At high temperatures, the structural correlation between the initial and any of the instantaneous structures (in thermal equilibrium) has been lost such that the cluster structure in this thermal region is disordered and shows a high atomic mobility, i.e., a liquid-like behavior. However, between low and high temperatures, the structural diversity of the potential energy surface emerges as a set of different isomeric structures.

These isomers exhibit solid-like behavior, maintaining atomic bonds and oscillating around the equilibrium position. However, their geometrical structures differ, and the atoms experience more energetic vibrations while remaining bounded. During this temperature range, the atomic cluster interacts with the external thermal environment, absorbing enough energy to induce intense atomic vibrations beyond the harmonic approximation. This permits the cluster to explore multiple minima of the corresponding PES. Consequently, as the MD simulation progresses, we can observe the occurrences of isomer hopping at different time intervals. The preceding description offers insight into how the energy landscape is explored in the course of a molecular dynamics simulation.<sup>32</sup>

Free or supported Pd clusters are important in the chemical industry mainly because of their catalytic activity for several chemical reactions, most notably, the methanol oxidation reaction (MOR). This chemical reaction holds a pivotal role in hydrogen production. Surprisingly, the size effect on the catalytic activity for Pd catalysts is in this reaction less significant than that of other metal nanocatalysts such as Pt, while methanol conversion and selectivity rise in response to the increase of reaction temperature.<sup>33</sup> Pd-based catalysts also show a low degree of catalyst poisoning in alkaline media.<sup>34</sup> Due to the relevance of the effect of temperature on the catalytic properties of Pd nanoparticles and the linear behavior found on the calculated caloric curve (see Figure 1), in this work, we analyze the thermal behavior of Pd<sub>8</sub> cluster performing BOMD computer simulations. This particular cluster size exhibits an exceptional degree of catalytic activity in CO oxidation, thus making this nanomaterial highly relevant for operation at room temperatures or higher. Theoretically, subnanometric clusters represent a challenge for describing phase transitions, using the thermodynamic principles typically applied to macroscopic systems. In this work, we also aim to show that computer simulation results align with the characteristics of melting observed in bulk materials.

In particular, we have explored the cluster's behavior across diverse thermal scenarios, which is essential to distinguish the potential manifestation of a solid–liquid phase transition in subnanometric metal clusters. Through this investigation, we aim to shed light on the interplay among temperature, structural stability, and potential energy landscape of the Pd<sub>8</sub> cluster, thereby unveiling significant implications for its application in catalytic processes. The methodology of this work is presented in Methodology, and results are given and discussed in Results and Discussion.

## 2. METHODOLOGY

The level of theory used for all DFT calculations using deMon2k was the PBE<sup>35,36</sup> functional in combination with a quasi-relativistic effective core-potential to describe the Pd atoms with 18 valence electrons (QECP18/SDD basis set). For the variational density fitting, the GEN-A2\*<sup>35</sup> auxiliary function set was used. In addition, for the frequency analysis, the analytical Hessian was calculated to obtain normal-mode frequencies. In this respect, deMon2k makes use of the analytic second derivatives from auxiliary density perturbation theory (ADPT), which removes the timings bottleneck due to its efficient parallelization scheme.<sup>37</sup> In terms of computational hardware, all calculations were carried out using 40 Intel(R) Xeon(R) Gold 6230 cores at 2.10 GHz available in our laboratory at the Universidad de Sonora.

A noteworthy detail about the structures used in this investigation is the comprehensive exploration of the Pd<sub>8</sub> cluster's low-energy geometrical configurations. This exhaustive search was performed using a locally developed code based on the basin-hopping (BH) method.<sup>38</sup> In this search, the cluster's PES was explored by the integration of the BH method in conjunction with the DFT scheme, as implemented in the Gaussian code.<sup>39</sup> The PBE functional in combination with the Stuttgart–Dresden (SDD) pseudopotentials and valence basis set<sup>40</sup> were employed for computations. Subsequently, the obtained structures were reoptimized in the framework of ADFT using the deMon2k code to obtain starting structures for BOMD simulations. The reoptimized structures were characterized by frequency analysis to validate the stability of the identified isomers, thus, ensuring the reliability of the obtained isomer configurations.

To study the temperature effect on the Pd<sub>8</sub> cluster, we used the BOMD scheme on top of the reoptimized structures in combination with the NVT canonical ensemble and a 3 chains Nosé–Hoover thermostat<sup>41</sup> with a frequency of 1500 cm<sup>-1</sup>. The BOMD simulations were carried out from an initial temperature of 100 until 2000 K. To assess the thermodynamic behavior of the Pd<sub>8</sub> cluster, the average internal energy was plotted as a function of the different temperatures to build the caloric curve. The atomic mean-square displacement (MSD) and the pair-distance distribution function (PDDF) were also calculated for the different temperatures in order to estimate the solid–liquid phase transition, i.e., the melting temperature. The distribution of distances between pairs of atoms is graphically illustrated by the PDDF, and the peaks in the function give important information about the degree of structural order in the material in any of its phases. It is important to note that changes in temperature can affect the peak position, height, and width in PDDF. For example, in crystalline solids, the first peak corresponds to the nearest-neighbor distance and is, therefore, sharp and well defined. In contrast, in liquids, this peak is broader and less well defined due to the lack of long-range order. A similar interpretation is applied to atomic clusters and nanoparticles to gain a deeper understanding of their structural changes as a function of temperature. From molecular dynamics simulations, the PDDF is obtained by calculating the distance between all atom pairs and binning them into a histogram. The selection of bin width in the histogram is a crucial consideration for obtaining informative distributions.

The peaks in the PDDF have been recognized as indicators of the coordination environment and local order in diverse nanomaterials. In particular, the vanishing of the second peak in the PDDF has been associated with a quasi-first-order phase transition in metal nanoparticles.<sup>42</sup> Additionally, to comprehensively identify all visited minima throughout the molecular dynamics simulations, a data clustering technique was applied to each BOMD trajectory using the OPTICS algorithm as implemented in scikit-learn.<sup>43</sup> The ordering points to identify the clustering structure (OPTICS) algorithm produces a hierarchical organization of the data based on density, and has the ability to identify clusters within data that display different densities.<sup>44</sup> At the beginning of the algorithm, a point is chosen at random, and its reachability distance is updated. The reachability distance is a measure of the minimum distance required for a given data point to be directly reachable from another data point. This metric quantifies the density of the data points within the neighborhood. Specifically, the reachability distance of a data point is determined by the larger value of two

factors: (1) the distance between the data point and its nearest neighbor and (2) a predetermined distance threshold known as the  $\varepsilon$  value. This represents the maximum distance at which a data point can still be considered to be part of the same cluster. In the OPTICS algorithm, the reachability distance is used to arrange the data points in a reachability plot, which visualizes the clustering structure of the data. Points with smaller reachability distances are considered core points, while those with larger reachability distances are classified as outliers or noise points. The algorithm proceeds by selecting the next point with the highest reachability distance and updating the distances of its neighboring points. This process is repeated until all points had been processed. By leveraging the reachability distance metric, we arranged the data points to enable spatially proximal points to be neighbors in the ordering. Points that are part of a cluster exhibit a low reachability distance to their nearest neighbor. As a result, data clusters are represented as valleys in the reachability plot. In molecular dynamics simulations, regions of the PES that experience a higher visitation frequency result in areas with denser data. These high-density regions correspond to distinct energy basins. By leveraging the clustering of the trajectory data, it becomes feasible to pinpoint these high-density areas and subsequently identify the isomers explored during each simulation.

Another indicative measure of a melting transition is the mean-square displacement (MSD), which quantifies the mobility of cluster atoms. The displacement ( $\Delta r_i(t)$ ) of each particle  $i$  over a given time  $t$  is tracked throughout the entire simulation time ( $K$ ), and subsequently, the average square of these displacements is plotted against time<sup>45</sup>

$$\langle \Delta r_i(t)^2 \rangle = \frac{1}{K} \sum_{i=1}^K \Delta r_i(t)^2 \quad (1)$$

In this equation,  $\Delta r(t)$  is the distance one of the atoms in the cluster travels at in time  $t$ . For the low-energy states, the atomic mobility occurs primarily around equilibrium positions (vibrations), resulting in MSD constant values over time. As the energy increases, atoms undergo more extensive movement, causing atomic vibrations to extend beyond the harmonic approximation. This can lead to complex phenomena such as isomer hopping and surface melting in clusters, and around a characteristic temperature, bulk atoms initiate diffusion, marking the transition to a fluid-like state. Within this high-energy regime, the MSD increases linearly with time. This is due to the tendency of the MD method to approximate the Brownian motion in the high-temperature limit. Under this condition, the atoms have higher kinetic energies and the frequency of collisions among them is increased. As a result, their motion becomes more random and, from this perspective, diffusion can be perceived as a process resembling a random walk, wherein each atom undergoes a random displacement during each time step. This behavior contributes to the linear increase of the MSD with respect to time.

Once the temperature for the possible melting of Pd<sub>8</sub> was determined, a parallel-tempering BOMD<sup>46</sup> with 32 replicas between 300 and 800 K was performed. The setup was identical to the single trajectory BOMDs, with a time step of 1 fs and a simulation length of 200 ps. Replica exchange was attempted every 100 time steps.

### 3. RESULTS AND DISCUSSION

Table 1 reports relative energies for the optimized putative global minimum structure of Pd<sub>8</sub>, a trigonal dodecahedron, with

**Table 1. Relative Energies,  $\Delta E$ , Lowest Frequencies,  $\omega_e$ , and Zero-Point Energies, ZPE, for Singlet, Triplet, Quintet, and Septet Optimized Trigonal Dodecahedron Putative Minimum Structures of Pd<sub>8</sub>**

multiplicity	$\Delta E$ [kcal/mol]	$\omega_e$ [cm <sup>-1</sup> ]	ZPE [kcal/mol]
1	1.4	63.4	3.5
3	0.9	61.3	3.3
5	0.0	69.0	3.4
7	10.6	68.8	3.4

different multiplicities. As this table shows, the quintet trigonal dodecahedron is lowest in energy. Quasi-degenerated to this structure are the corresponding triplet and singlet structures. Topologically, all of these structures are almost identical. On the other hand, the septet structure is energetically well separated from the three low-lying multiplicities.

Figure 2 illustrates the computed PDDF of the lowest-energy Pd<sub>8</sub> cluster over a range of temperatures. Notably, there is a

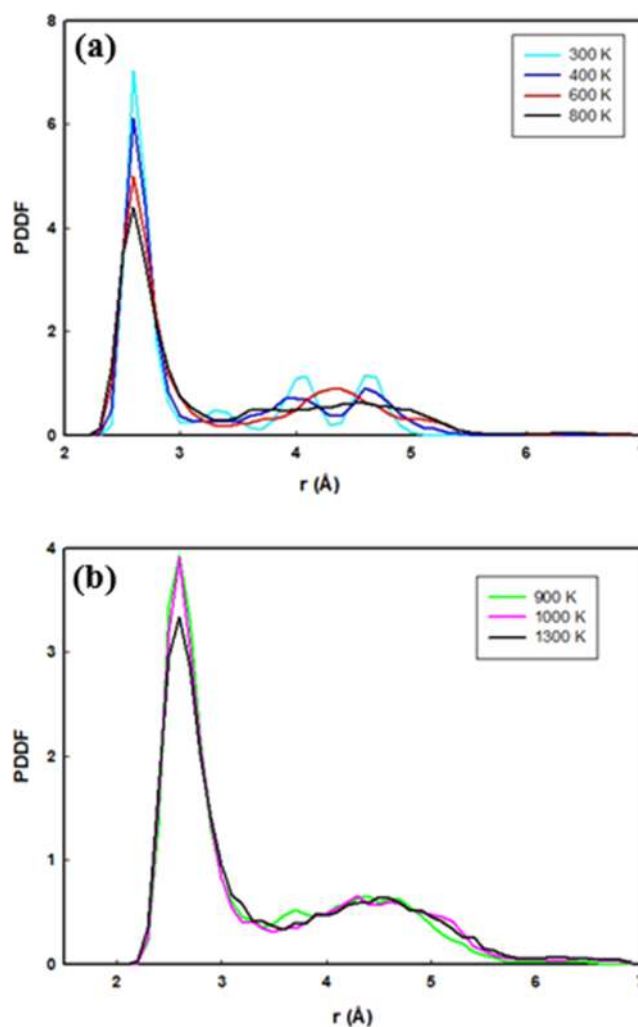


**Figure 2.** PDDF calculated from BOMD trajectories in the temperature ranges (a) 300–800 K and (b) 900–1300 K. The second peak vanishes at 400 K, and the liquid-like behavior appears above 600 K.

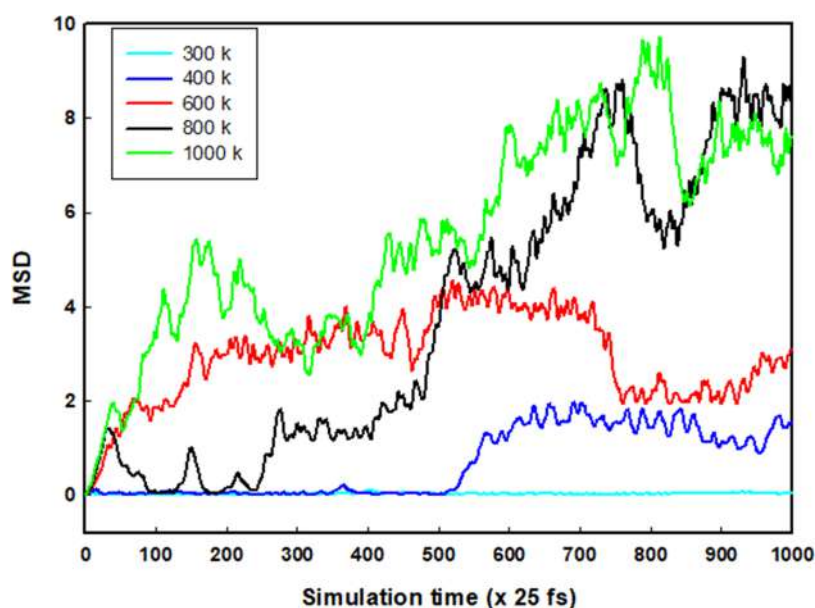


Figure 3. MSD behavior showing the Pd<sub>8</sub> cluster dynamical behavior in the temperature range 300–1000 K.

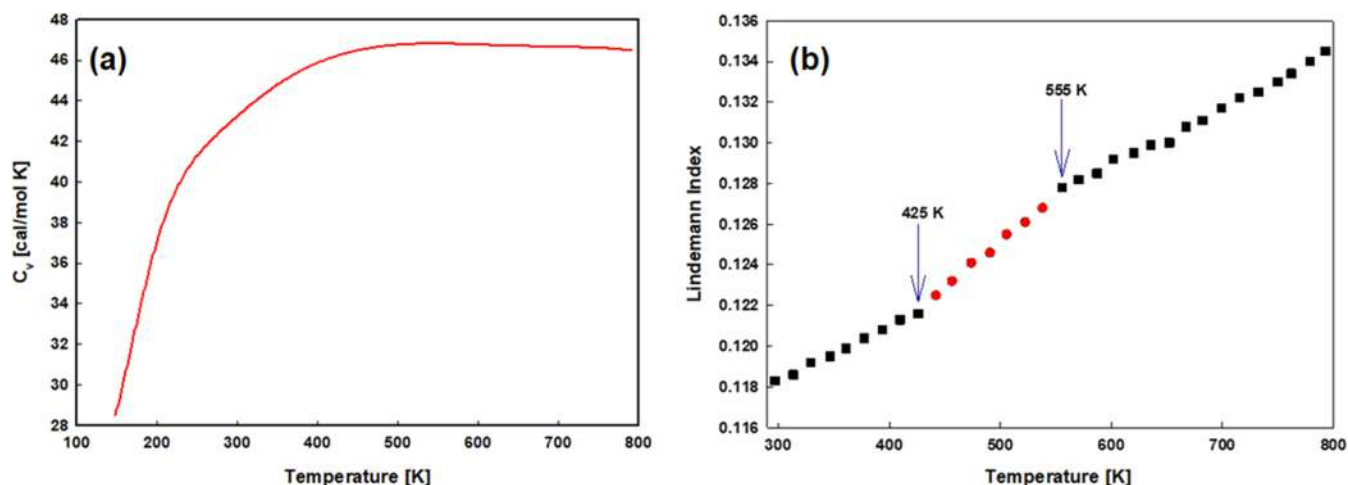


Figure 4. (a) Heat capacity curve obtained from parallel-tempering MD and (b) Lindemann parameter calculated from BOMD simulations. In (b), the arrows show approximately the competition zone between the melting and isomerization processes.

pronounced reduction in the intensity of the first peak as the temperature is raised.

At 300 K, we can observe a peak emerging at around 3.3 Å, signifying a specific atomic arrangement for this small cluster. However, this distinctive peak apparently vanishes as the temperature rises to 400 K. This change strongly suggests a structural rearrangement, solid–solid- or solid–liquid-like, occurring within the temperature range of 300–400 K. During this structural change, the atoms' mobility increases due to an increase in the internal energy. However, the characteristic profile of PDDF resembling the liquid behavior in macroscopic systems is observed above 600 K (red line). This result implies that relying solely on the disappearance of the second peak of PDDF may not be sufficient for detecting phase transitions in clusters of this small size. Nonetheless, it does offer utility in identifying the transition zone where isomerization remains viable. To elucidate whether these new atomic arrangements are liquid-like or, alternatively, higher-energy isomers, we computed the MSD at different temperatures. These results are depicted in Figure 3.

The Pd<sub>8</sub> cluster exhibits isomer hopping within the transition zone (ca. 400–500 K), which is characterized by distinctive plateau-like regions in the MSD plots. At the same time from around 500 K, a shift toward liquid-like behavior might appear. Thus, cluster melting is in competition with isomerization. To gain further insight into this competition, we recorded 32 200 ps trajectories from parallel-tempering BOMD. To ease computational demand, we used the singlet multiplicity in this study. Using the multiple-histogram method,<sup>47</sup> we obtained the heat capacity curve depicted in the left graph of Figure 4. It shows a broad maximum between 400 and 600 K. This indicates a finite system melting transition which is further supported by the corresponding Lindemann parameter<sup>48</sup> plot shown in the right graph of Figure 4.

The dynamical behavior of the Pd<sub>8</sub> cluster clearly reveals the solid behavior within the lower temperature range from 100 to 400 K, while showcasing a shift toward liquid-like behavior at temperatures above. Interestingly, the plateau-like shape in MSD appears at 600 K (red curve in Figure 3) after a short simulation time that exhibits liquid-like behavior, i.e., a linear

increase of MSD. There is an interesting transition region, where a variety of isomer structures appear to coexist. In this transition region, thermal oscillations and atomic mobility facilitate interchanges between potential energy minima. This behavior is intricately linked to temperature, which provides sufficient energy to surmount energy barriers, enabling transitions between different minima, i.e., isomer hopping. Our approach to localizing isomers is based on BOMD simulations, as previously stated. Nevertheless, different methodologies may be utilized to distinguish the various isomers of the metal clusters at finite temperature.<sup>49,50</sup>

The existence of different isomers at finite temperatures was confirmed by a constant-energy BOMD simulation using the PBE/SDD level of theory in the NVT scheme. Figure 5

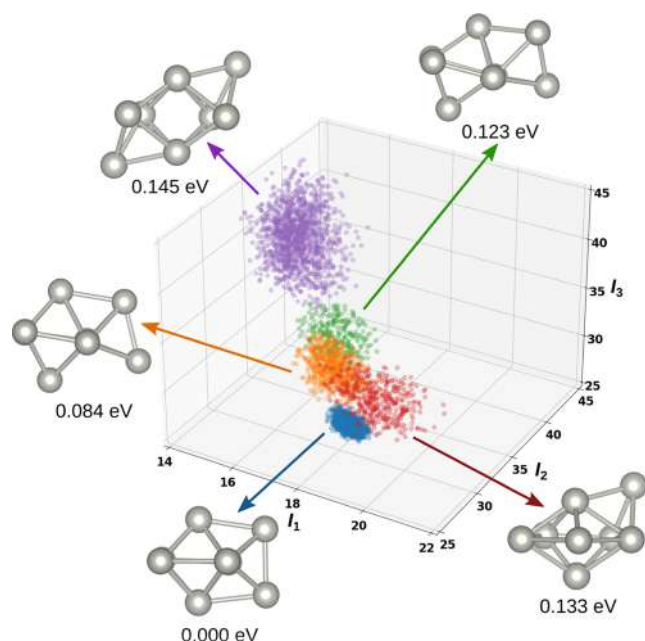


**Figure 5.** Scatter plot of the data clustering analysis determining the high-density zones where different isomers can be found. The axes represent the principal moments of inertia (in atomic units) of the clusters. Different colors represent the energy regions in which the isomers are located.

illustrates the outcomes of our data clustering analysis, strategically identifying high-density zones within which different isomers are situated. Each data point on the plot corresponds to a specific isomer of the Pd<sub>8</sub> cluster. Importantly, it should be noted that while the isomers shown are not optimized configurations, they are in reasonable agreement with those obtained by Luna-Valenzuela et al.<sup>51</sup> using the PBE and PBE0 functionals to explore the potential energy surface through an ab initio basin-hopping global search algorithm.

The data clustering analysis applied to the combined BOMD trajectories at different temperatures revealed the existence of five distinct Pd<sub>8</sub> isomers, as depicted in Figure 5. This observation suggests that these clusters undergo significant structural changes, leading from one low-energy isomer to the subsequent higher-energy isomer as the temperature increases. This graphical depiction offers valuable insights into the energetic distribution of the isomers, found in the BOMD trajectories at a given temperature, facilitating a comprehensive understanding of their prevalence and occurrence within the scrutinized data set.

A more detailed illustration of the interplay between temperature, Pd<sub>8</sub> cluster structure, and isomerization is given in Figure 6. Here, a detailed perspective on the evolving distribution of isomers in response to temperature changes is apparent. At lower temperatures (<200 K), the structure exhibits oscillations predominantly around the global minimum. As the temperature rises, diverse isomers emerge, each with their own distinctive features. It is worth noting that once the temperature surpasses the 800 K threshold (illustrated by the red line), these structures cease to visit their respective energy basins, i.e., the depth valleys in the plots decrease. Moreover, by 1300 K (represented by the brown line), the structure assumes an essentially disordered configuration.

At temperatures of 600 and 800 K, it is observed that isomeric structures including the trigonal dodecahedron, capped pentagonal bipyramid, and a distorted elongated structure emerge throughout the simulations. However, their prevalence, indicated by the extent of high-density zones, is notably higher at 600 K, as depicted in the corresponding graphs in Figure 6. On the other hand, at 800 K, the incidence of the trigonal dodecahedron structure (first valley) remains significant. We believe that there exists a correlation between isomer prevalence and the behavior of the MSD curve, but further studies are needed to validate this connection. Nonetheless, this figure clearly illustrates that the competition between isomer hopping and melting occurring at high temperatures decreases as the temperature rises.

For the Pd<sub>8</sub> cluster, the process of isomerization initiates at approximately 300 K. At this temperature, the cluster attains sufficient energy to surmount the energy barriers separating different isomers, thus fluctuating between the lowest-energy isomer and the subsequent higher-energy isomer. As the temperature further increases, this cluster undergoes various structural transformations among different configurations (isomers), and at significantly elevated temperatures, though still below the bulk melting point, the cluster's atoms display unhindered diffusion across the structure, resulting in a disordered appearance akin to liquid behavior.<sup>52</sup> The broad maximum in the heat capacity curve indicates a competition between cluster melting and isomerization. This is also highlighted by the fact that multiple energy minima are visited during a BOMD simulation at a finite temperature, thus establishing a rational connection between temperature and the complex potential energy landscape.

#### 4. CONCLUSIONS

To gain insight into the effect of temperature on the Pd<sub>8</sub> cluster's structure, BOMD simulations were performed at different temperatures. Employing PDDF, we discerned its suitability as an indicator of the structural change occurring in the studied temperature range for a small metal cluster. The existence of a structural change was determined through the vanishing of the second peak of this function. This observation was complemented by analyzing the MSD computed at various temperatures. This analysis aided in determining that the melting features of the Pd<sub>8</sub> cluster emerge at approximately 500 K, which manifests itself by a broad maximum in the heat capacity curve starting at this temperature. To investigate isomerization in Pd<sub>8</sub> as the temperature increases, we analyzed the total energy of the cluster at various thermal regimes. Our results revealed that at low temperatures, the cluster primarily exhibits vibrational motion around its lowest-energy minimum, i.e., the initial configuration. However, structural transformations occur within

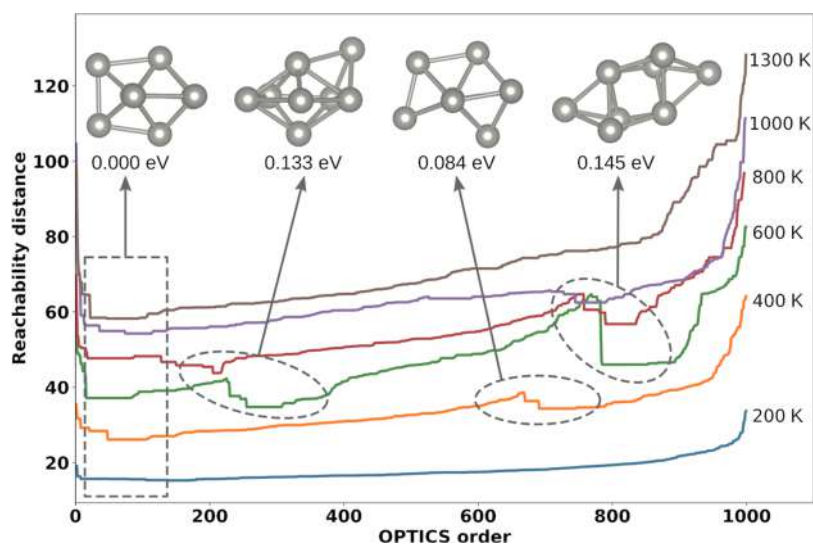


**Figure 6.** Reachability plot obtained from the OPTICS data clustering analysis at different temperatures. The valleys, delimited by dashed figures, are visual indicators of high-density zones within data and indicate the localization of distinct isomers in the BOMD trajectories (Supporting Information). Note that the reachability distance grows with increasing temperature.

an intermediate temperature range, leading to the identification of distinct isomeric structures. Through meticulous clustering of the BOMD trajectories, we have successfully delineated regions of high data point concentration, indicating the presence of distinct isomeric arrangements within the transition zone and prior to the melting transition. Overall, this approach reveals the complex melting patterns that occur in small metal clusters. Thus, cluster isomerization competes with the cluster melting in  $\text{Pd}_8$ . As a result, a rather broad maximum in the heat capacity curve is found.

In conclusion, a comprehensive methodology encompassing both static and dynamic data obtained from BOMD simulations is essential for discerning the transition between solid-like and liquid-like phases. This methodology, coupled with a meticulous analysis of the molecular dynamics trajectory at different temperatures, such as that provided by the data clustering approach employed in this work, is essential when subnanometric clusters are investigated.

## ■ ASSOCIATED CONTENT

### SI Supporting Information

The Supporting Information is available free of charge at <https://pubs.acs.org/doi/10.1021/acs.jpca.3c06173>.

400 (MOL)

600 (MOL)

800 (MOL)

Cartesian coordinates (in Å) of the atoms corresponding to four  $\text{Pd}_8$  isomers observed during the BOMD simulations; BOMD trajectory files corresponding to temperatures 400, 600, and 800 K (DOCX)

## ■ AUTHOR INFORMATION

### Corresponding Author

Alvaro Posada-Amarillas – *Departamento de Investigación en Física, Universidad de Sonora, 83000 Hermosillo, Sonora, México*; [orcid.org/0000-0001-7533-4820](https://orcid.org/0000-0001-7533-4820);  
Email: [posada@cifus.uson.mx](mailto:posada@cifus.uson.mx)

## Authors

Analía Luna-Valenzuela – *Departamento de Ciencias de la Salud, Unidad Regional Los Mochis, Universidad Autónoma de Occidente, 81217 Los Mochis, Sinaloa, México*

Jesús N. Pedroza-Montero – *Departamento de Química, CINVESTAV, Av. Instituto Politécnico Nacional, 2508 Ciudad de México, México*; [orcid.org/0000-0001-6528-4700](https://orcid.org/0000-0001-6528-4700)

Andreas M. Köster – *Departamento de Química, CINVESTAV, Av. Instituto Politécnico Nacional, 2508 Ciudad de México, México*; [orcid.org/0000-0001-9279-3455](https://orcid.org/0000-0001-9279-3455)

Patrizia Calaminici – *Departamento de Química, CINVESTAV, Av. Instituto Politécnico Nacional, 2508 Ciudad de México, México*; [orcid.org/0000-0001-9842-4271](https://orcid.org/0000-0001-9842-4271)

Luis E. Gálvez-González – *Departamento de Investigación en Física, Universidad de Sonora, 83000 Hermosillo, Sonora, México*; [orcid.org/0000-0002-4614-3520](https://orcid.org/0000-0002-4614-3520)

Complete contact information is available at:

<https://pubs.acs.org/10.1021/acs.jpca.3c06173>

## Notes

The authors declare no competing financial interest.

## ■ ACKNOWLEDGMENTS

A.P.A. and A.M.K. acknowledge funding from Conacyt through grants A1-S-39326 and A1-S-11929, respectively. This work was supported by the ECOS project 321168. The parallel-tempering BOMD runs were performed at the Compute Canada HPC facility NARVAL under the resource allocation project ban-780-ae.

## ■ REFERENCES

- Baletto, F.; Ferrando, R. Structural Properties of Nanoclusters: Energetic, Thermodynamic, and Kinetic Effects. *Rev. Mod. Phys.* **2005**, *77* (1), 371 DOI: [10.1103/RevModPhys.77.371](https://doi.org/10.1103/RevModPhys.77.371).
- Védrine, J. C. Metal Oxides in Heterogeneous Oxidation Catalysis: State of the Art and Challenges for a More Sustainable

- World. *ChemSusChem* **2019**, *12* (3), 577–588, DOI: 10.1002/cssc.201802248.
- (3) Johnston, R. L. *Atomic and Molecular Clusters* Taylor and Francis: London and New York, 2002.
- (4) Gaston, N. Cluster Melting: New, Limiting, and Liminal Phenomena. *Adv. Phys.: X* **2018**, *3* (1), No. 1401487, DOI: 10.1080/23746149.2017.1401487.
- (5) Schön, J. C.; Putz, H.; Jansen, M. Studying the Energy Hypersurface of Continuous Systems-The Threshold Algorithm. *J. Phys.: Condens. Matter* **1996**, *8* (2), 143 DOI: 10.1088/0953-8984/8/2/004.
- (6) Doye, J. P. K.; Wales, D. J. Thermodynamics of Global Optimization. *Phys. Rev. Lett.* **1998**, *80* (7), 1357 DOI: 10.1103/PhysRevLett.80.1357.
- (7) Heiles, S.; Johnston, R. L. Global Optimization of Clusters Using Electronic Structure Methods. *Int. J. Quantum Chem.* **2013**, *113* (18), 2091–2109, DOI: 10.1002/qua.24462.
- (8) Lourenço, M. P.; Barrios Herrera, L.; Hostaš, J.; Calaminici, P.; Köster, A. M.; Tchagang, A.; Salahub, D. R. QMLMaterial-A Quantum Machine Learning Software for Material Design and Discovery. *J. Chem. Theory Comput.* **2023**, *19* (17), 5999–6010, DOI: 10.1021/acs.jctc.3c00566.
- (9) Foster, D. M.; Ferrando, R.; Palmer, R. E. Experimental Determination of the Energy Difference between Competing Isomers of Deposited, Size-Selected Gold Nanoclusters. *Nat. Commun.* **2018**, *9* (1), No. 1323, DOI: 10.1038/s41467-018-03794-9.
- (10) Maneri, A. H.; Singh, C. P.; Kumar, R.; Maibam, A.; Krishnamurty, S. Mapping the Finite-Temperature Behavior of Conformations to Their Potential Energy Barriers: Case Studies on Si<sub>6</sub>B and Si<sub>7</sub>B Clusters. *ACS Omega* **2022**, *7* (7), 6167–6173, DOI: 10.1021/acsomega.1c06654.
- (11) Fiscaro, G.; Schaefer, B.; Finkler, J. A.; Goedecker, S. Principles of Isomer Stability in Small Clusters. *Mater. Adv.* **2023**, *4* (7), 1746–1768, DOI: 10.1039/D2MA01088G.
- (12) Garzón, I.; Michaelian, K.; Beltrán, M. R.; Posada-Amarillas, A.; Ordejón, P.; Artacho, E.; Sánchez-Porta, L. D.; Soler, J. M. Structure and Thermal Stability of Gold Nanoclusters: The Au<sub>38</sub> case. *Eur. Phys. J. D* **1999**, *9*, 211–215.
- (13) Cabrera-Trujillo, J. M.; Montejano-Carrizales, J. M.; Aguilera-Granja, F.; Posada-Amarillas, A. Theoretical Study of the Thermally Induced Structural Fluctuations in Sub-Nanometre Size Gold Clusters. *Eur. Phys. J. D* **2015**, *69*, 1–9, DOI: 10.1140/epjd/e2015-60058-y.
- (14) Sanders-Gutierrez, O. A.; Luna-Valenzuela, A.; Posada-Borbón, A.; Schön, J. C.; Posada-Amarillas, A. Molecular Dynamics and DFT Study of 38-Atom Coinage Metal Clusters. *Comput. Mater. Sci.* **2022**, *201*, No. 110908.
- (15) Taherkhani, F.; Fortunelli, A. Chemical Ordering and Temperature Effects on the Thermal Conductivity of Ag–Au and Ag–Pd Bimetallic Bulk and Nanocluster Systems. *New J. Chem.* **2022**, *46* (40), 19213–19229, DOI: 10.1039/D2NJ02899A.
- (16) Luna-Valenzuela, A.; Cabellos, J. L.; Posada-Amarillas, A. Effect of Temperature on the Structure of Pd<sub>8</sub> and Pd<sub>7</sub>Au<sub>1</sub> Clusters: An Ab Initio Molecular Dynamics Approach. *Theor. Chem. Acc.* **2021**, *140* (7), 86 DOI: 10.1007/s00214-021-02771-8.
- (17) Carroll, L. L.; Moskaleva, L. V.; de Lara-Castells, M. P. Carbon Vacancy-Assisted Stabilization of Individual Cu<sub>5</sub> Clusters on Graphene. Insights from *ab initio* Molecular Dynamics. *Phys. Chem. Chem. Phys.* **2023**, *25*, 15729–15743, DOI: 10.1039/D2CP05843J.
- (18) Castleman, A. W., Jr; Harms, A. C.; Leuchtner, R. E. Gas Phase Reactivity of Thermal Metal Clusters. *Z. Phys. D: At., Mol. Clusters* **1991**, *19*, 343–346.
- (19) Calaminici, P.; Alvarez-Ibarra, A.; Cruz-Olvera, D.; Domínguez-Soria, V. D.; Flores-Moreno, R.; Gamboa, G. U.; Geudtner, G.; Goursot, A.; Mejía-Rodríguez, D.; Salahub, D. R. et al. Auxiliary Density Functional Theory: From Molecules to Nanostructures. In *Handbook of Computational Chemistry*; Leszczynski, J. et al., Ed.; Springer International Publishing: Switzerland, 2016; p 1.
- (20) Köster, A. M.; Geudtner, G.; Calaminici, P.; Casida, M. E.; Domínguez-Soria, V. D.; Flores-Moreno, R.; Gamboa, G. U.; Goursot, A.; Heine, T.; Ipatov, A. et al. *deMon2k Version 3*; The deMon developers: Cinvestav, Mexico City, 2011 <http://www.demon-software.com/>.
- (21) Krishnamurty, S.; Shafai, G. S.; Kanhere, D. G.; et al. Ab Initio Molecular Dynamical Investigation of the Finite Temperature Behavior of the Tetrahedral Au<sub>19</sub> and Au<sub>20</sub> Clusters. *J. Phys. Chem. A* **2007**, *111* (42), 10769–10775, DOI: 10.1021/jp075896+.
- (22) De, H. S.; Krishnamurty, S.; Mishra, D.; Pal, S. Finite Temperature Behavior of Gas Phase Neutral Au<sub>n</sub> (3 ≤ n ≤ 10) Clusters: A First Principles Investigation. *J. Phys. Chem. C* **2011**, *115* (35), 17278–17285, DOI: 10.1021/jp2023605.
- (23) De, H. S.; Krishnamurty, S.; Pal, S. A First Principle Investigation on the Thermal Stability of a Golden Fullerene: A Case Study of Au<sub>32</sub>. *Catal. Today* **2012**, *198* (1), 106–109, DOI: 10.1016/j.cattod.2012.04.072.
- (24) Vásquez-Pérez, J. M.; Gamboa, G. U.; Mejía-Rodríguez, D.; Alvarez-Ibarra, A.; Geudtner, G.; Calaminici, P.; Köster, A. M. Influence of Spin Multiplicity on the Melting of Na<sub>55</sub><sup>+</sup>. *J. Phys. Chem. Lett.* **2015**, *6* (22), 4646–4652, DOI: 10.1021/acs.jpcllett.5b01983.
- (25) Joshi, K.; Krishnamurti, S. Au<sub>26</sub>: A Case of Fluxionality/Co-Existence. *Phys. Chem. Chem. Phys.* **2018**, *20* (13), 8616–8623, DOI: 10.1039/C7CP07997D.
- (26) Vásquez-Pérez, J. M.; Köster, A. M.; Calaminici, P. The Melting Limit in Sodium Clusters. *Theor. Chem. Acc.* **2018**, *137* (3), 45 DOI: 10.1007/s00214-018-2210-7.
- (27) Sun, J. J.; Cheng, J. Solid-to-Liquid Phase Transitions of Sub-Nanometer Clusters Enhance Chemical Transformation. *Nat. Commun.* **2019**, *10* (1), No. 5400, DOI: 10.1038/s41467-019-13509-3.
- (28) Fan, Q. Y.; Wang, Y.; Cheng, J. Size-Sensitive Dynamic Catalysis of Subnanometer Cu Clusters in CO<sub>2</sub> Dissociation. *J. Phys. Chem. Lett.* **2021**, *12* (16), 3891–3897, DOI: 10.1021/acs.jpcllett.1c00506.
- (29) Pittalis, S.; Proetto, C. R.; Floris, A.; Sanna, A.; Bersier, C.; Burke, K.; Gross, E. K. U. Exact Conditions in Finite-Temperature Density-Functional Theory. *Phys. Rev. Lett.* **2011**, *107* (16), 163001 DOI: 10.1103/PhysRevLett.107.163001.
- (30) Chen, B. J.; Chai, J. D. TAO-DFT Fictitious Temperature Made Simple. *RSC Adv.* **2022**, *12* (19), 12193–12210, DOI: 10.1039/D2RA01632J.
- (31) Valsson, O.; Parrinello, M. Thermodynamical Description of a Quasi-First-Order Phase Transition from the Well-Tempered Ensemble. *J. Chem. Theory Comput.* **2013**, *9* (12), 5267–5276, DOI: 10.1021/ct400859f.
- (32) Wales, D. J.; Berry, R. S. Coexistence in Finite Systems. *Phys. Rev. Lett.* **1994**, *73* (21), 2875 DOI: 10.1103/PhysRevLett.73.2875.
- (33) Ubago-Pérez, R.; Carrasco-Marín, F.; Moreno-Castilla, C. Methanol Partial Oxidation on Carbon-Supported Pt and Pd Catalysts. *Catal. Today* **2007**, *123* (1-4), 158–163, DOI: 10.1016/j.cattod.2007.02.014.
- (34) Maya-Cornejo, J.; Ledesma-Durán, A.; Hernández, S. I.; Santamaría-Holek, I. Competitive Adsorption and Interplay between Methanol and Water During Electro-Oxidation on Pd-Based Electrocatalyst. *J. Electrochem. Soc.* **2022**, *169* (4), No. 046505, DOI: 10.1149/1945-7111/ac6321.
- (35) Perdew, J. P.; Burke, K.; Ernzerhof, M. Generalized Gradient Approximation Made Simple. *Phys. Rev. Lett.* **1996**, *77* (18), 3865 DOI: 10.1103/PhysRevLett.77.3865.
- (36) Calaminici, P.; Janetzko, F.; Köster, A. M.; Mejía-Olvera, R.; Zuniga-Gutierrez, B. Density Functional Theory Optimized Basis Sets for Gradient Corrected Functionals: 3d Transition Metal Systems. *J. Chem. Phys.* **2007**, *126* (4), No. 044108, DOI: 10.1063/1.2431643.
- (37) Delgado-Venegas, R. I.; Mejía-Rodríguez, D.; Flores-Moreno, R.; Calaminici, P.; Köster, A. M. Analytical Second Derivatives from Auxiliary Density Perturbation Theory. *J. Chem. Phys.* **2016**, *145* (22), No. 224103, DOI: 10.1063/1.4971292.
- (38) Wales, D. J.; Doye, J. P. K. Global Optimization by Basin-Hopping and the Lowest Energy Structures of Lennard-Jones Clusters Containing up to 110 Atoms. *J. Phys. Chem. A* **1997**, *101* (28), 5111–5116, DOI: 10.1021/jp970984n.

(39) Frisch, M. J.; Trucks, G. W.; Schlegel, H. B.; Scuseria, G. E.; Robb, M. A.; Cheeseman, J. R.; Scalmani, G.; Barone, V.; Petersson, G. A.; Nakatsuji, H. et al. *Gaussian 09*, Revision D.01; Gaussian, Inc.: Wallingford CT, 2016.

(40) Dolg, M.; Cao, X. Relativistic Pseudopotentials: Their Development and Scope of Applications. *Chem. Rev.* **2012**, *112* (1), 403–480, DOI: [10.1021/cr2001383](https://doi.org/10.1021/cr2001383).

(41) Gamboa, G. U.; Vásquez-Pérez, J. M.; Calaminici, P.; Köster, A. M. The Influence of Thermostats on the Calculation of Heat Capacities from Born-Oppenheimer Molecular Dynamics Simulations. *Int. J. Quantum Chem.* **2010**, *110* (12), 2172–2178, DOI: [10.1002/qua.22518](https://doi.org/10.1002/qua.22518).

(42) Delgado-Callico, L.; Rossi, K.; Pinto-Miles, R.; Salzbrenner, P.; Baletto, F. Universal Signature in the Melting of Metallic Nanoparticles. *Nanoscale* **2020**, DOI: [10.1039/D0NR06850K](https://doi.org/10.1039/D0NR06850K).

(43) Pedregosa, F.; Varoquaux, G.; Gramfort, A.; Michel, V.; Thirion, B.; Grisel, O.; Blondel, M.; Prettenhofer, P.; Weiss, R.; Dubourg, V.; et al. Scikit-learn: Machine Learning in Python. *J. Mach. Learn. Res.* **2011**, *12*, 2825–2830.

(44) Ankerst, M.; Breunig, M. M.; Kriegel, H.-P.; Sander, J. SIGMOD/PODS99: International Conference on Management of Data and Symposium on Principles of Database Systems, Philadelphia, Pennsylvania, USA *OPTICS: Ordering Points to Identify the Clustering Structure*; ACM Press: New York, NY, 1999.

(45) Frenkel, D.; Smit, B. *Understanding Molecular Dynamics*, 2nd ed.; Academic Press: Amsterdam, 2002; Vol. 638, pp 192–196.

(46) Louisonard, F.; Geudnter, G.; Köster, A. M.; Cuny, J. Implementation of the Parallel-tempering Molecular Dynamics Method in deMon2k and Application to the Water Hexamer. *Theor. Chem. Acc.* **2021**, *140* (7), 95 DOI: [10.1007/s00214-021-02765-6](https://doi.org/10.1007/s00214-021-02765-6).

(47) Ferrenberg, A. M.; Swendsen, R. H. Optimized Monte Carlo Data Analysis. *Phys. Rev. Lett.* **1989**, *63* (12), 1195 DOI: [10.1103/PhysRevLett.63.1195](https://doi.org/10.1103/PhysRevLett.63.1195).

(48) Beck, T. L.; Doll, J. D.; Freeman, D. L. The Quantum Mechanics of Cluster Melting. *J. Chem. Phys.* **1989**, *90* (10), 5651–5656, DOI: [10.1063/1.456687](https://doi.org/10.1063/1.456687).

(49) Grigoryan, V. G.; Springbor, M. Temperature and Isomeric Effects in Nanoclusters. *Phys. Chem. Chem. Phys.* **2019**, *21* (10), 5646–5654, DOI: [10.1039/C9CP00123A](https://doi.org/10.1039/C9CP00123A).

(50) Settem, M.; Roncaglia, C.; Ferrando, R.; Giacomello, A. Structural Transformations in Cu, Ag, and Au Metal Nanoclusters. *J. Chem. Phys.* **2023**, *159* (9), No. 094303, DOI: [10.1063/5.0159257](https://doi.org/10.1063/5.0159257).

(51) Luna-Valenzuela, A.; Cabellos, J. L.; Alonso, J. A.; Posada-Amarillas, A. Effects of van der Waals Interactions on the Structure and Stability of Cu<sub>8-x</sub>Pd<sub>x</sub> (x = 0, 4, 8) Cluster Isomers. *Mater. Today Commun.* **2021**, *26*, No. 102024.

(52) Garzón, I. L.; Jellinek, J. Peculiarities of Structures and Meltinglike Transition in Gold Clusters. *Z. Phys. D: At, Mol. Clusters* **1993**, *26*, 316–318.